CHAPTER 4.

Drought and Moisture Surplus Patterns in the Conterminous United States: 2017, 2015—2017, and 2013—2017

Frank H. Koch
John W. Coulston

INTRODUCTION

Although droughts affect most U.S. forests, there is considerable variation between regions in terms of drought frequency and intensity (Hanson and Weltzin 2000). These differences characterize the regions' prevailing drought regimes. Most forests in the Western United States are subject to annual seasonal droughts. In contrast, forests in the Eastern United States usually experience one of two general drought patterns: random (i.e., occurring at any time of year) occasional droughts, as observed in the Appalachian Mountains and the Northeast, or frequent late-summer droughts, as usually observed in the Southeastern Coastal Plain and the eastern portion of the Great Plains (Hanson and Weltzin 2000).

In forests, moisture scarcity during droughts can result in significant tree stress, particularly when that scarcity is accompanied by high temperatures (L.D.L. Anderegg and others 2013, Peters and others 2015, Williams and others 2013). Trees and other plants respond to this stress by decreasing fundamental growth processes (e.g., cell division and enlargement). Because photosynthesis is less sensitive than these fundamental processes, it decreases slowly at low levels of drought stress, but decreases more quickly as drought stress increases in severity (Kareiva and others 1993, Mattson and Haack 1987). Besides these direct effects, drought stress often makes trees vulnerable to attack by damaging insects and diseases (Clinton and others 1993, Kolb and others 2016, Mattson and Haack 1987, Raffa and others 2008). Droughts also exacerbate wildland fire risk by limiting breakdown of organic matter and reducing the moisture content of downed woody debris and other potential fire fuels (Clark 1989, Keetch and Byram 1968, Schoennagel and others 2004, Trouet and others 2010).

Generally, forest systems are resistant to short-term droughts, although individual tree species differ in their ability to tolerate drought conditions (Archaux and Wolters 2006, Berdanier and Clark 2016). Because of this resistance, drought duration may be more important for forests than intensity (Archaux and Wolters 2006). For example, forests that experience multiple consecutive years of drought (2–5 years) are much more likely to exhibit high tree mortality than forests that experience a single year of extreme drought (Guarín and Taylor 2005, Millar and others 2007). Therefore, a thorough evaluation of drought impact in forests should include analysis of moisture conditions over multiyear time windows.

In the 2010 Forest Health Monitoring (FHM) National Technical Report, we described a method for mapping drought conditions across the conterminous United States (Koch and others 2013b). Our objective was to generate fine-scale, drought-related spatial datasets that improve upon similar products available from sources such as the National Climatic Data Center (e.g., Vose and others 2014) or the U.S. Drought Monitor program (Svoboda and others 2002). The principal inputs are gridded climate data (i.e., monthly raster maps of precipitation

and temperature over a 100-year period) created with the Parameter-elevation Regression on Independent Slopes (PRISM) climate mapping system (Daly and others 2002). The method utilizes a standardized indexing approach that facilitates comparison of a given location's moisture status during different time windows, regardless of their length. The index is easier to calculate than the commonly used Palmer Drought Severity Index, or PDSI (Palmer 1965), and avoids some criticisms of the PDSI (see Alley 1984) regarding its underlying assumptions and limited comparability across space and time. Here, we applied the method outlined in the 2010 FHM Report to the most currently available climate data (i.e., the monthly PRISM data through 2017), thereby providing the ninth installment in an ongoing series of annual drought assessments for the conterminous United States from 2009 forward (Koch and Coulston 2015, 2016, 2017, 2018; Koch and others 2013a, 2013b, 2014, 2015).

This is the fourth year in which we also mapped levels of moisture surplus across the conterminous United States during multiple time windows. While recent refereed literature (e.g., Adams and others 2009, Allen and others 2010, Martínez-Vilalta and others 2012, Peng and others 2011, Williams and others 2013) has focused more often on reports of regional-scale forest decline and mortality due to persistent drought conditions, especially in combination with periods of extremely high temperatures (i.e., heat waves), surplus moisture availability can also be detrimental to forests. Abnormally high moisture can be a short-term stressor (e.g., an extreme rainfall event with subsequent flooding) or a long-term stressor (e.g., persistent wetness driven by a macroscale climatic pattern such as the El Niño-Southern Oscillation), either of which may lead to tree dieback and mortality (Rozas and García-González 2012, Rozas and Sampedro 2013). Such impacts have been observed in both tropical and temperate forests (Hubbart and others 2016, Laurance and others 2009, Rozas and García-González 2012). While surplus-induced impacts in forests may not be as common as drought-induced impacts, a single index that depicts both moisture surplus and deficit conditions provides a fuller accounting of potential forest health issues.

METHODS

We acquired grids for monthly precipitation and monthly mean temperature for the conterminous United States from the PRISM Climate Group Web site (PRISM Climate Group 2018). At the time of these analyses, gridded datasets were available for all years from 1895 to 2017. However, the grids for December 2017 were only provisional versions (i.e., finalized grids had not yet been released). For analytical purposes, we treated these provisional grids as if they were the final versions. The spatial resolution of the grids was approximately 4 km (cell area = 16 km^2). For future applications and to ensure better compatibility with other spatial datasets, all output grids were resampled to a spatial resolution of approximately 2 km (cell area = 4 km^2) using a nearest neighbor

approach. The nearest neighbor approach is a computationally simple resampling method that avoids the smoothing of data values observed with methods such as bilinear interpolation or cubic convolution.

Potential Evapotranspiration (PET) Maps

As in our previous drought mapping efforts (Koch and Coulston 2015, 2016, 2017, 2018; Koch and others 2012a, 2012b, 2013a, 2013b, 2014, 2015), we adopted an approach in which a moisture index value is calculated for each location of interest (i.e., each grid cell in a map of the conterminous United States) during a given time period. Moisture indices are intended to reflect the amount of available water in a location (e.g., to support plant growth). In our case, the index is computed using an approach that considers both the amount of precipitation that falls on a location during the period of interest as well as the level of potential evapotranspiration during this period. Potential evapotranspiration measures the loss of soil moisture through plant uptake and transpiration (Akin 1991). It does not measure actual moisture loss, but rather the loss that would occur if there was no possible shortage of moisture for plants to transpire (Akin 1991, Thornthwaite 1948). In simple terms, potential evapotranspiration serves as a measure of moisture demand. By including potential evapotranspiration along with precipitation, our index thus documents the long-term balance between moisture demand and supply for each location of interest.

To complement the available PRISM monthly precipitation grids, we computed corresponding monthly potential evapotranspiration (*PET*) grids using Thornthwaite's formula (Akin 1991, Thornthwaite 1948):

$$PET_m = 1.6 L_{lm} (10 \frac{T_m}{I})^a \qquad (1)$$

where

PET_m = the potential evapotranspiration for a given month m in cm

L_{lm} = a correction factor for the mean possible duration of sunlight during month m for all locations (i.e., grid cells) at a particular latitude l [see Table V in Thornthwaite (1948) for a list of L correction factors by month and latitude]

T_m = the mean temperature for month m in degrees C

I = an annual heat index, calculated as

$$I = \sum_{m=1}^{12} \left(\frac{T_m}{5} \right)^{1.514}$$

where

T_m is the mean temperature for each month m of the year

a = an exponent calculated as $a = 6.75 \times 10^{-7} I^3 - 7.71 \times 10^{-5} I^2 + 1.792 \times 10^{-2} I + 0.49239$ [see Appendix I in Thornthwaite (1948) regarding calculation of I and the empirical derivation of a]

Although only a simple approximation, a key advantage of Thornthwaite's formula is that it has modest input data requirements (i.e., mean temperature values) compared to more sophisticated methods of estimating PET such as the Penman-Monteith equation (Monteith 1965), which requires less readily available data on factors such as humidity, radiation, and wind speed. To implement equation (1) spatially, we created a grid of latitude values for determining the L adjustment for any given grid cell (and any given month) in the conterminous United States. We extracted the T_m values for the grid cells from the corresponding PRISM mean monthly temperature grids.

Moisture Index Maps

To estimate baseline conditions, we used the precipitation (P) and PET grids to generate moisture index grids for the past 100 years (i.e., 1918–2017) for the conterminous United States. We used a moisture index described by Willmott and Feddema (1992), which has been applied in a variety of contexts, including global vegetation modeling (Potter and Klooster 1999) and climate change analysis (Grundstein 2009). Willmott and Feddema (1992) devised the index as a refinement of one described earlier by Thornthwaite (1948) and Thornthwaite and Mather (1955). Their revised index, MI', has the following form:

$$MI' = \begin{cases} P/PET - 1 & , \quad P < PET \\ 1 - PET/P & , \quad P \geq PET \\ 0 & , \quad P = PET = 0 \end{cases} \qquad (2)$$

where

P = precipitation

PET = potential evapotranspiration, as calculated using equation (1)

(P and PET must be in equivalent measurement units, e.g., mm)

This set of equations yields a symmetric, dimensionless index scaled between -1 and 1. A primary advantage of this symmetry is that it enables valid comparisons between any set of locations in terms of their moisture balance (i.e., the balance between moisture demand and supply). MI' can be calculated for any time period, but is commonly calculated on an annual basis using P and PET values summed across the entire year (Willmott and Feddema 1992). An alternative to this summation approach is to

calculate MI' on a monthly basis (i.e., from total measured precipitation and estimated potential evapotranspiration in each month), and then, for a given time window of interest, calculate its moisture index as the mean of the MI' values for all months in the time window. This "mean-of-months" approach limits the ability of short-term peaks in either precipitation or potential evapotranspiration to negate corresponding short-term deficits, as would happen under a summation approach.

For each year in our study period (i.e., 1918–2017), we used the mean-of-months approach to calculate moisture index grids for three different time windows: 1 year (MI_1'), 3 years (MI_3'), and 5 years (MI_5'). Briefly, the MI_1' grids are the mean (i.e., the mean value for each grid cell) of the 12 monthly MI' grids for each year in the study period, the MI_3' grids are the mean of the 36 monthly grids from January of 2 years prior through December of the target year, and the MI_5' grids are the mean of the 60 consecutive monthly MI' grids from January of 4 years prior to December of the target year. Thus, the MI_1' grid for the year 2017 is the mean of the monthly MI' grids from January to December 2017, while the MI_3' grid is the mean of the grids from January 2015 to December 2017, and the MI_5' grid is the mean of the grids from January 2013 to December 2017.

Annual and Multiyear Drought Maps

To determine degree of departure from typical moisture conditions, we first created a normal grid, $MI'_{i\ norm}$, for each of our three time windows, representing the mean (i.e., the mean value for each grid cell) of the 100 corresponding moisture index grids (i.e., the MI_1', MI_3', or MI_5' grids, depending on the window; see fig. 4.1). We also created a standard deviation grid, $MI'_{i\ SD}$, for each time window, calculated from the window's 100 individual moisture index grids as well as its $MI'_{i\ norm}$ grid. We subsequently calculated moisture difference z-scores, MDZ_{ij}, for each time window using these derived datasets:

$$MDZ_{ij} = \frac{MI_i' - MI_{i\ norm}'}{MI_{i\ SD}'} \qquad (3)$$

where

i = the analytical time window (i.e., 1, 3, or 5 years)

j = a particular target year in our 100-year study period (i.e., 1918–2017)

MDZ scores may be classified in terms of degree of moisture deficit or surplus (table 4.1). The classification scheme includes categories (e.g., severe drought, extreme drought) like

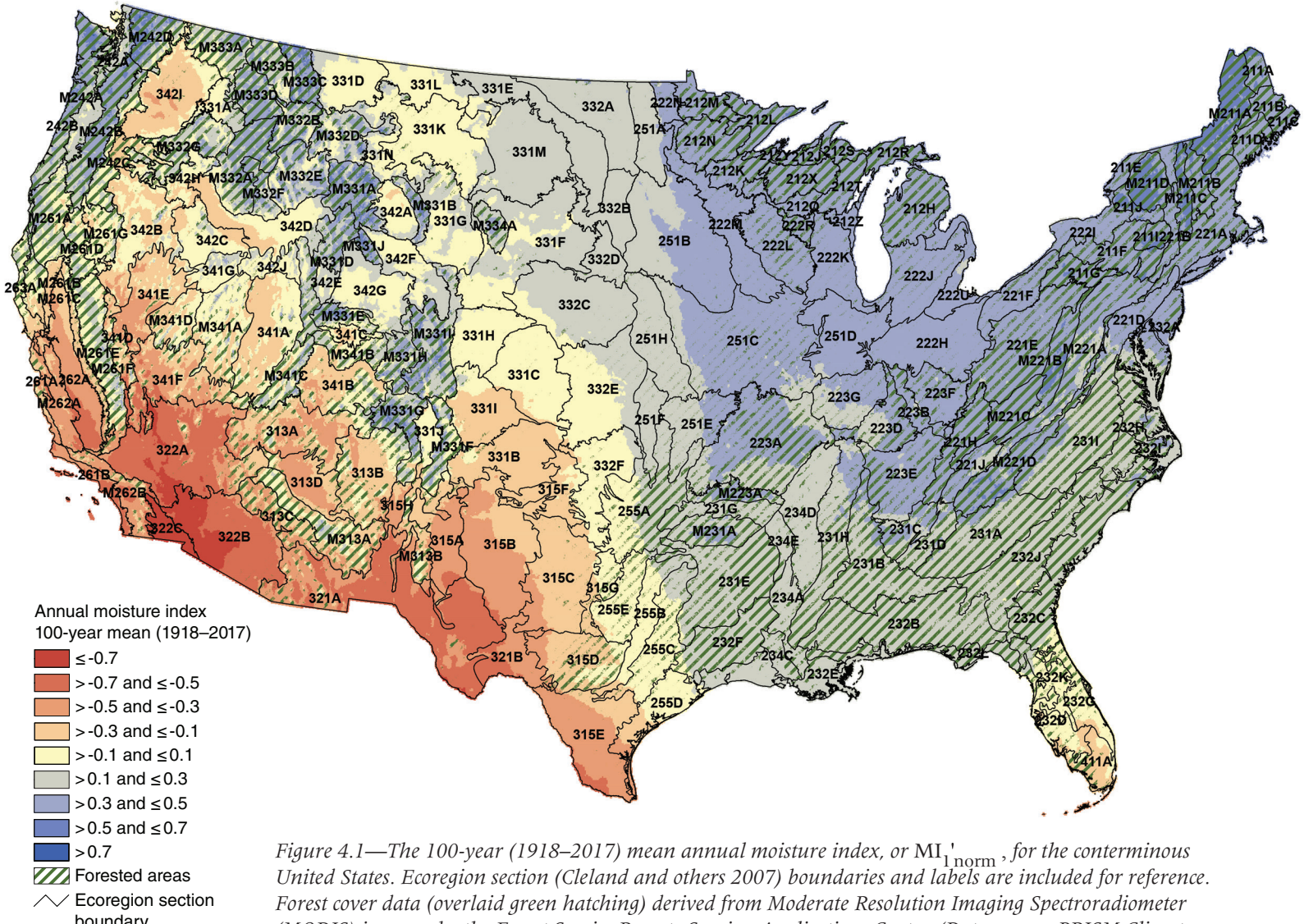

Figure 4.1—The 100-year (1918–2017) mean annual moisture index, or $MI_{1'norm}$, *for the conterminous United States. Ecoregion section (Cleland and others 2007) boundaries and labels are included for reference. Forest cover data (overlaid green hatching) derived from Moderate Resolution Imaging Spectroradiometer (MODIS) imagery by the Forest Service Remote Sensing Applications Center. (Data source: PRISM Climate Group, Oregon State University)*

Table 4.1—Moisture difference *z*-score (*MDZ*) value ranges for nine wetness and drought categories, along with each category's approximate theoretical frequency of occurrence

Score	Category	Frequency
MDZ ≤ -2	Extreme drought	2.3%
-2 < MDZ ≤ -1.5	Severe drought	4.4%
-1.5 < MDZ ≤ -1	Moderate drought	9.2%
-1 < MDZ ≤ -0.5	Mild drought	15%
-0.5 < MDZ ≤ 0.5	Near normal conditions	38.2%
0.5 < MDZ ≤ 1	Mild moisture surplus	15%
1 < MDZ ≤ 1.5	Moderate moisture surplus	9.2%
1.5 < MDZ ≤ 2	Severe moisture surplus	4.4%
MDZ > 2	Extreme moisture surplus	2.3%

those associated with the PDSI. The scheme has also been adopted for other drought indices such as the Standardized Precipitation Index, or SPI (McKee and others 1993). Moreover, the breakpoints between *MDZ* categories resemble those used for the SPI, such that we expect the *MDZ* categories to have theoretical frequencies of occurrence that are similar to their SPI counterparts (e.g., approximately 2.3 percent of the time for extreme drought; see McKee and others 1993, Steinemann 2003). More importantly, because of the standardization in equation (3), the breakpoints between categories remain the same regardless of the size of the time window of interest. For comparative analysis, we generated and classified *MDZ* maps of the conterminous United States, based on all three time windows, for the target year 2017.

RESULTS AND DISCUSSION

The 100-year (1918–2017) mean annual moisture index, or $MI_{1}'_{norm}$, grid (fig. 4.1) provides an overview of moisture regimes in the conterminous United States. (The 100-year $MI_{3}'_{norm}$ and $MI_{5}'_{norm}$ grids were similar to the mean $MI_{1}'_{norm}$ grid, and so are not shown here.) Wet climates ($MI' > 0$) are typical in the Eastern United States, especially the Northeast. An interesting anomaly is southern Florida, primarily ecoregion sections (Cleland and others 2007) 232D–Florida Coastal Lowlands-Gulf, 232G–Florida Coastal Lowlands-Atlantic, and 411A–Everglades. This region appears to be dry relative to other parts of the East, which is an effect of its tropical climate, which has distinct wet (primarily summer months) and dry (late fall to early spring) seasons. Although southern Florida usually receives a high level of precipitation during the wet season, it can be insufficient to offset the region's lengthy dry season (Duever and others 1994) or its high level of temperature-driven evapotranspiration, especially during the late spring and summer months, resulting in negative MI' values.

The climatic regime of southern Florida contrasts markedly with the pattern observed in the driest parts of the Western United States, particularly the Southwest (e.g., sections 322A–Mojave Desert, 322B–Sonoran Desert, and 322C–Colorado Desert), where potential evapotranspiration is very high, but precipitation levels are typically very low. In fact, because

of generally lower precipitation than the East, dry climates (*MI′* <0) are typical across much of the Western United States. Nevertheless, mountainous areas in the central and northern Rocky Mountains as well as the Pacific Northwest are relatively wet, such as ecoregion sections M242A–Oregon and Washington Coast Ranges, M242B–Western Cascades, M331G–South Central Highlands, and M333C–Northern Rockies. This is driven in part by large amounts of winter snowfall in these regions (Hanson and Weltzin 2000).

Figure 4.2 shows the annual (i.e., 1-year) *MDZ* map for 2017 for the conterminous United States. Although there are areas of mild to extreme drought (*MDZ* ≤-0.5) scattered across the country, the most distinctive feature of the map is a large contiguous zone of extreme drought (*MDZ* ≤-2) in the Southwestern United States. Encompassing virtually the entire "Four Corners" region (southeastern Utah, southwestern Colorado, northwestern New Mexico, and northeastern Arizona), this contiguous zone extended into at least 18 ecoregion sections, including most of 313A–Grand Canyon, 313B–Navajo Canyonlands, 313D–Painted Desert, and M313A–White Mountains-San Francisco Peaks-Mogollon Rim. Although only M313A is predominately forested, all forested areas in 313A, 313B, and 313D experienced extreme drought conditions in 2017, as was similarly the case in 341B–Northern Canyonlands. Other forested ecoregion sections that fell partly in this contiguous zone include 313C–Tonto Transition and M341B–Tavaputs Plateau. To the south and west of the zone, extreme drought also occurred in the few isolated areas of forest within 321A–Basin and Range, 322A–Mojave Desert, and 341F–Southeastern Great Basin.

Severe to extreme drought conditions (*MDZ* ≤-1.5) affected forests in two ecoregion sections in southern California in 2017: almost all of M262B–Southern California Mountain and Valley as well as the southern portion of M261E–Sierra Nevada. Additionally, a few sizeable contiguous areas of mild to extreme drought occurred in the Midwestern United States. One of these areas affected sections 223G–Central Till Plains-Oak Hickory, 251C–Central Dissected Till Plains, 251D–Central Till Plains and Grand Prairies, as well as the heavily forested 223A–Ozark Highlands. A similar drought area to the west of this fell mostly in sections 332E–South Central Great Plains and 332F–South Central and Red Bed Plains, neither of which contains much forest. A third area along the Canadian border affected portions of 251A–Red River Valley, 331E–Northeastern Glaciated Plains, 331K–North Central Highlands, 331L–Glaciated Northern Highlands, 331M–Missouri Plateau, and 332A (also Northeastern Glaciated Plains); these ecoregion sections contain almost no forest cover.

The 1-year *MDZ* map for 2017 (fig. 4.2) is dramatically different from the 1-year map for 2016 (fig. 4.3). Many of the drought-affected areas that were prominent in the 2016 map saw improved moisture conditions during 2017. Perhaps most notably, the large area of

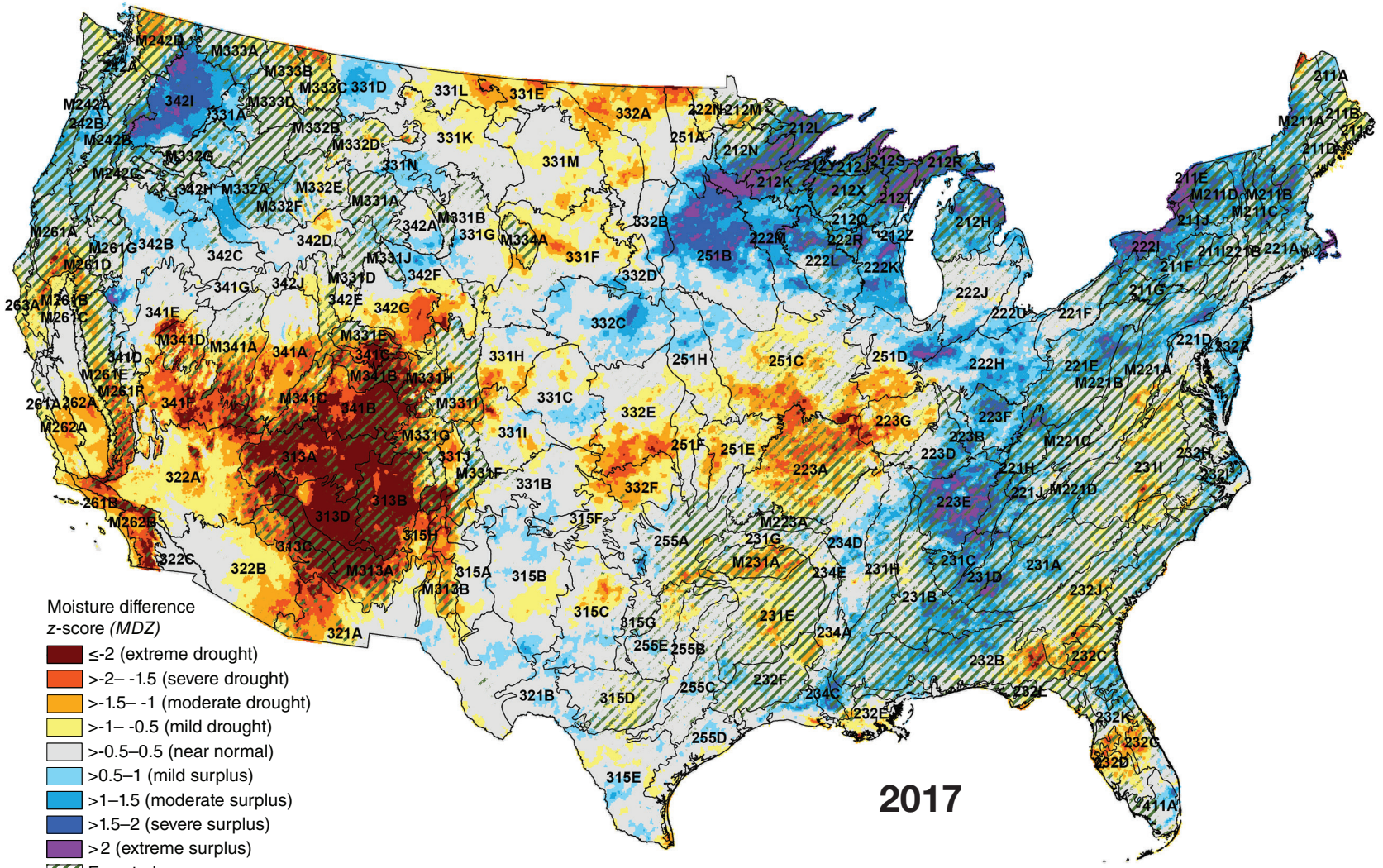

Figure 4.2—The 2017 annual (i.e., 1-year) moisture difference z-score, or MDZ, *for the conterminous United States. Ecoregion section (Cleland and others 2007) boundaries and labels are included for reference. Forest cover data (overlaid green hatching) derived from MODIS imagery by the Forest Service Remote Sensing Applications Center. (Data source: PRISM Climate Group, Oregon State University)*

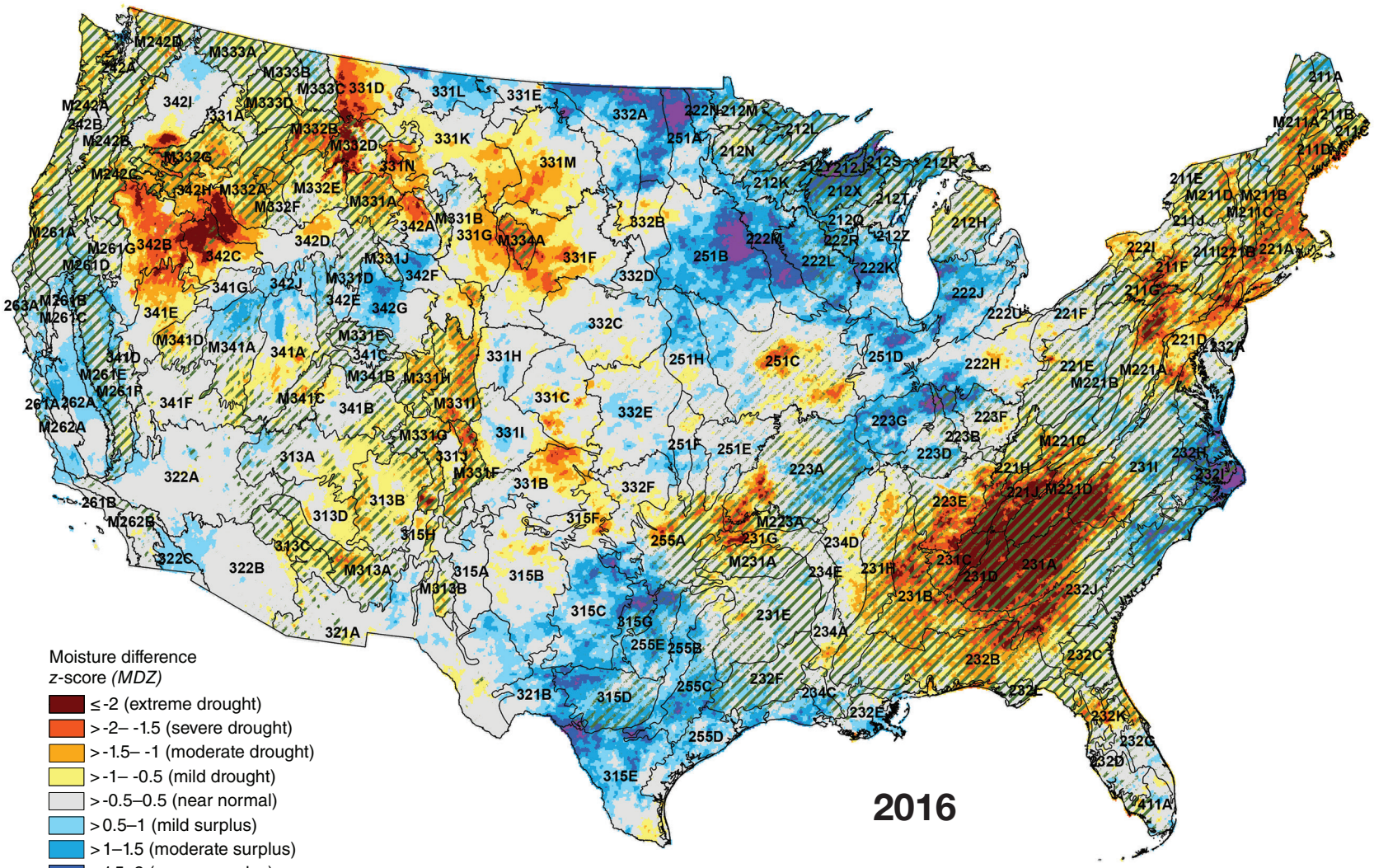

Figure 4.3—The 2016 annual (i.e., 1-year) moisture difference z-score, or MDZ, *for the conterminous United States. Ecoregion section (Cleland and others 2007) boundaries and labels are included for reference. Forest cover data (overlaid green hatching) derived from MODIS imagery by the Forest Service Remote Sensing Applications Center. (Data source: PRISM Climate Group, Oregon State University)*

severe to extreme drought that covered much of the Southeastern United States in 2016 (including forested sections 221H–Northern Cumberland Plateau, 221J–Central Ridge and Valley, 231A–Southern Appalachian Piedmont, 231C–Southern Cumberland Plateau, and 231D–Southern Ridge and Valley, as well as southern portions of M221D–Blue Ridge Mountains and 231I–Central Appalachian Piedmont) shifted to near normal or surplus conditions in 2017. Likewise, an area of mostly moderate to extreme drought that extended north from the Mid-Atlantic region into New England during 2016 contracted significantly in 2017, with drought conditions persisting only in portions of 211B–Maine-New Brunswick Foothills and Lowlands, 211C–Fundy Coastal and Interior, 211D–Central Maine Coastal and Embayment, and M211A–White Mountains. Unfortunately, most forested areas in California, which experienced near normal to surplus conditions in 2016 after several years of historically exceptional drought, saw drought conditions return in 2017, including the aforementioned severe to extreme drought in sections M262B–Southern California Mountain and Valley and M261E–Sierra Nevada. This return could magnify an already dramatic forest health impact: since 2010, an estimated 129 million trees have died in California due to direct or indirect drought effects (USDA Forest Service Region 5 Forest Health Monitoring program 2018).

The zone of extreme drought in the Four Corners region in 2017 represented an intensification and geographic expansion of mostly mild drought conditions that were present in 2016. As noted earlier (see fig. 4.1), high temperatures and low precipitation levels are regular features of the climatic regime of the Southwestern United States, so droughts of varying duration and intensity are common throughout the region. In recent years, however, temperatures in the Southwest have trended toward new highs compared to the historical record (i.e., since measurements began in 1895). For example, in Arizona and New Mexico, average temperatures in 2017 and in the corresponding 3-year (2015–2017) and 5-year (2013–2017) time periods were the warmest on record. In Colorado and Utah, 2017 was the third warmest year on record, while 2015–2017 and 2013–2017 were the warmest 3- and 5-year periods to date (National Climatic Data Center 2018b). Notably, none of these States received especially low levels of precipitation during these periods, other than a somewhat anomalous shortage of rainfall in late 2017 (National Climatic Data Center 2018a). Regardless, because climatological data and climate change projections suggest a continued warming trend globally—in terms of both average and extreme temperatures (Gil-Alana 2018, Rahmstorf and others 2017)—it is highly possible, if not likely, that drought impacts will worsen in the Southwest.

The 3-year (2015–2017; fig. 4.4) and 5-year (2013–2017; fig. 4.5) *MDZ* maps reveal other emerging drought patterns in the United States that may be linked to this warming trend. For instance, while droughts have been a persistent concern throughout much of the Western United States for the last several decades (Groisman and Knight 2008, Mueller and others 2005, Woodhouse and others 2010), it is only in the past few years that moderate to extreme drought conditions have been widespread in the Pacific Northwest, as shown in figures 4.4 and 4.5 (in particular, sections M332B–Northern Rockies and Bitterroot Valley, M333B–Flathead Valley, M333C–Northern Rockies, and M333D–Bitterroot Mountains). These conditions did not arise because of a lack of precipitation, but because warm temperatures disrupted the region's usual water balance; for example, winter precipitation fell as rain rather than snow, substantially reducing snowpack (Marlier and others 2017). Indeed, 2013–2017 was tied with 2012–2016 as the warmest 5-year period on record for the Pacific Northwest in terms of average temperatures (National Climatic Data Center 2018a).

Similarly, but on a smaller scale, the 3-year and 5-year *MDZ* maps show the persistence of drought conditions on New York's Long Island and in other portions of section 221A–Lower New England. Recently, this area has seen unprecedented outbreaks of the southern pine beetle (*Dendroctonus frontalis*), a native insect that has been associated historically with pine forests of the Southeastern United States. Although drought stress may be a weaker inciting factor for southern pine beetle activity than it is for other bark beetles (Kolb and others 2016), the emergence of the pest in an apparently novel environment has been linked to warming temperatures (Lesk and others 2017) that intensified drought conditions in the region (Sweet and others 2017). Furthermore, climate change projections suggest the beetle will expand farther into the Northeastern United States in the next few decades (Lesk and others 2017).

Broadly, the 3- and 5-year *MDZ* maps show differences between the Eastern and Western United States that are consistent with their disparate moisture regimes. As illustrated by the 3-year *MDZ* map (fig. 4.4), few forested areas west of the Great Plains experienced near normal or surplus moisture conditions during 2015–2017; indeed, only a handful of ecoregion sections could be characterized as mostly—but not completely—drought-free (e.g., M331D–Overthrust Mountains). By comparison, many forested areas east of the Rocky Mountains were essentially drought-free during this period. Indeed, other than the area in southern New England described previously, these areas of severe to extreme drought were usually restricted to the Southeastern United States (although areas of mild drought were reasonably widespread in the East). Moreover, these severe to extreme drought areas were less prominent in the 5-year *MDZ* map (fig. 4.5) than in the 3-year map (fig. 4.4), which indicates that these conditions developed primarily within

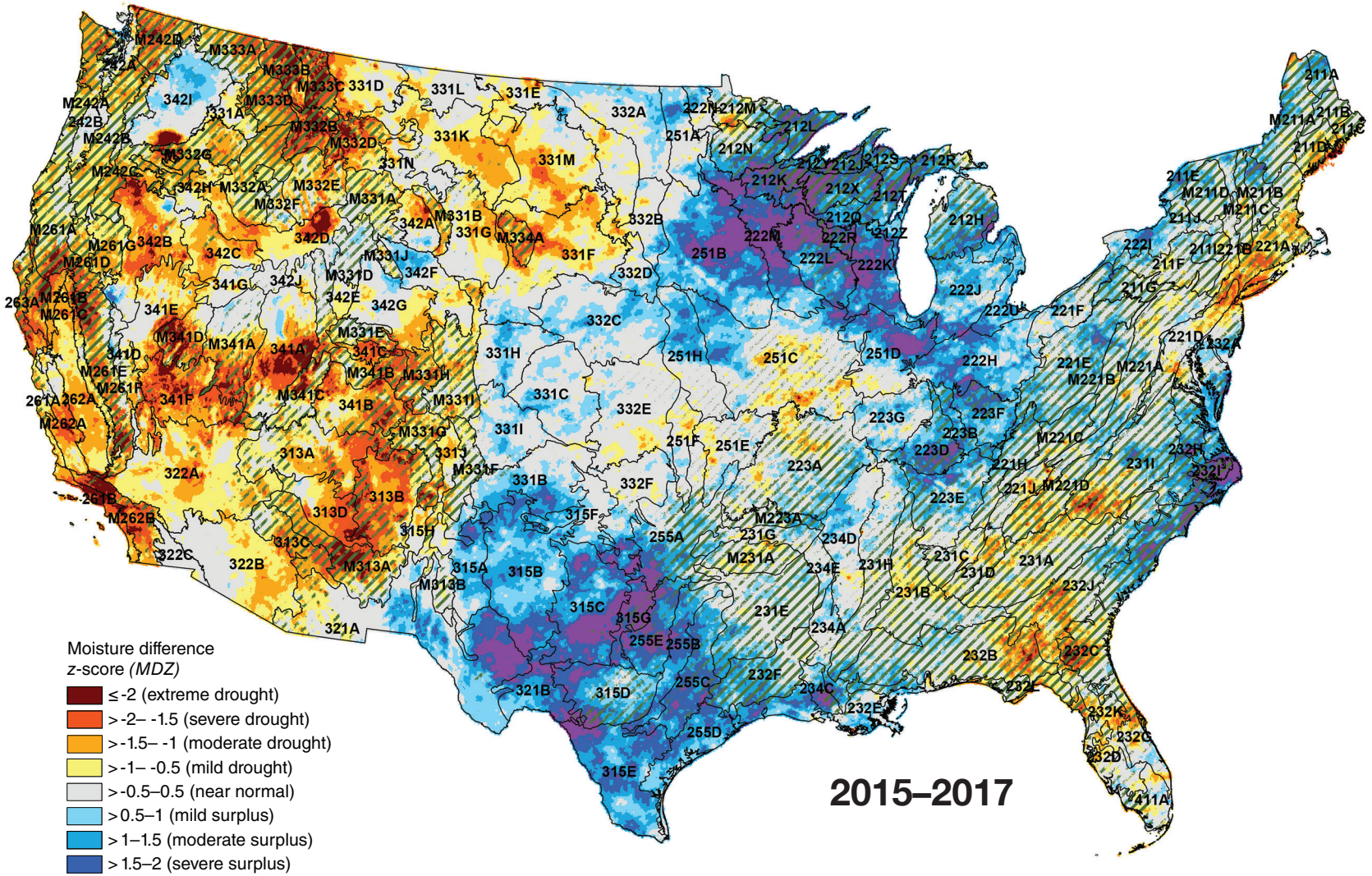

Figure 4.4—The 2015–2017 (i.e., 3-year) moisture difference z-score (MDZ) *for the conterminous United States. Ecoregion section (Cleland and others 2007) boundaries are included for reference. Forest cover data (overlaid green hatching) derived from MODIS imagery by the Forest Service Remote Sensing Applications Center. (Data source: PRISM Climate Group, Oregon State University)*

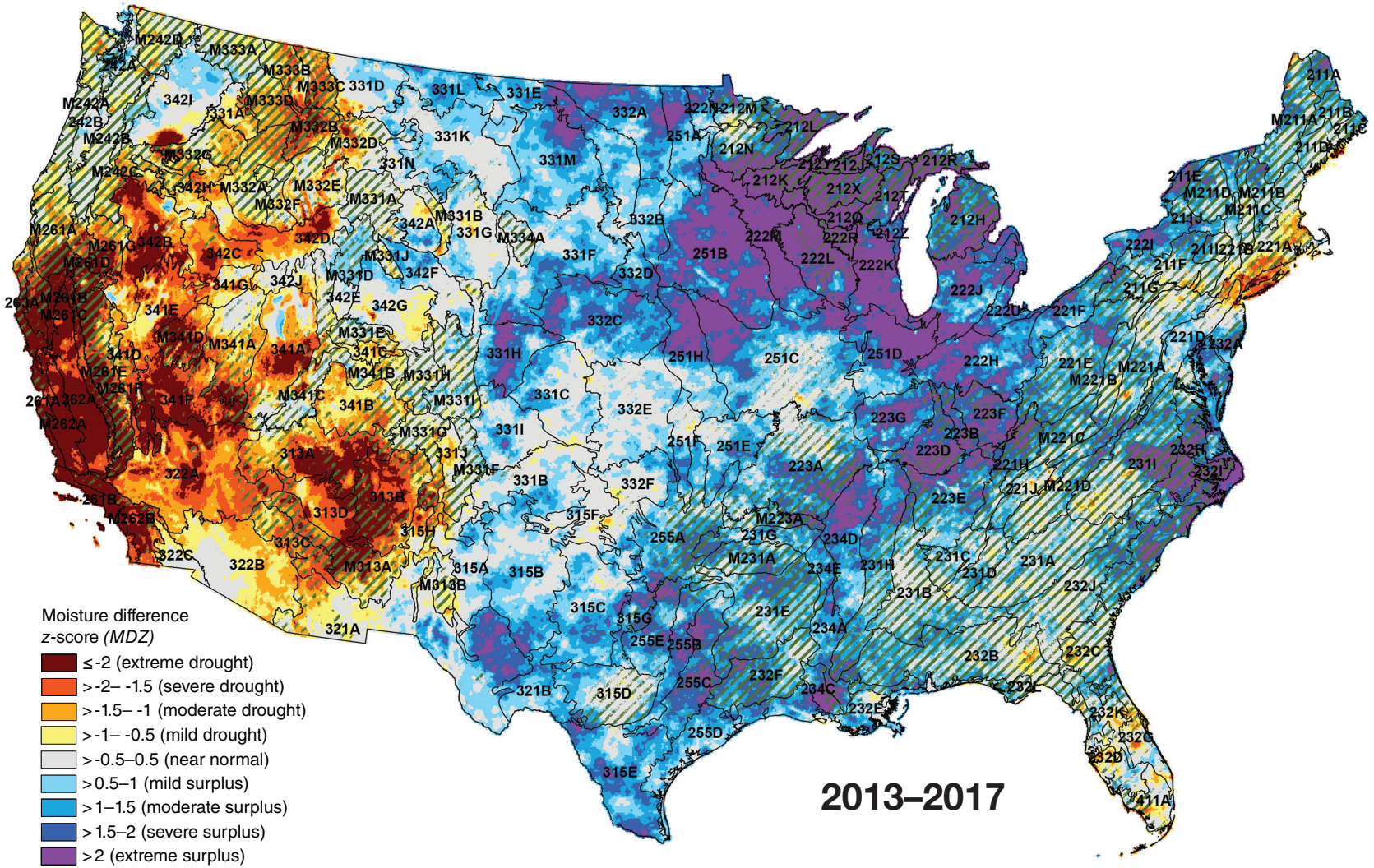

Figure 4.5—The 2013–2017 (i.e., 5-year) moisture difference z*-score (*MDZ*) for the conterminous United States. Ecoregion section (Cleland and others 2007) boundaries are included for reference. Forest cover data (overlaid green hatching) derived from MODIS imagery by the Forest Service Remote Sensing Applications Center. (Data source: PRISM Climate Group, Oregon State University)*

the last few years, and likely were preceded by near normal moisture conditions in 2013–2014. For example, one area in section 231I–Central Appalachian Piedmont can mostly be traced to the large contiguous zone of severe to extreme drought that occurred in 2016 (fig. 4.3). Another area in the southern portion of 232C–Atlantic Coastal Flatwoods appears to be linked to conditions that emerged primarily in 2017 (fig. 4.2).

Nevertheless, the contrast between the East and West is perhaps most emphasized by areas of moisture surplus documented in the 3-year and 5-year *MDZ* maps. While areas with severe to extreme surpluses were widespread east of the Rocky Mountains, they were virtually nonexistent west of the range. In particular, a few areas of surplus that appeared in the 5-year *MDZ* map (fig. 4.5) are worth highlighting: in the western Great Lakes region (especially forested sections 212J–Southern Superior Uplands, 212K–Western Superior Uplands, 212Q–North Central Wisconsin Uplands, 212R–Eastern Upper Peninsula, 212X–Northern Highlands, 212Y–Southwest Lake Superior Clay Plain, 222L–North Central U.S. Driftless and Escarpment, and 222R–Wisconsin Central Sands); in Kentucky and southern Indiana (223B–Interior Low Plateau-Transition Hills, 223D–Interior Low Plateau-Shawnee Hills, and 223F–Interior Low Plateau-Bluegrass); and in eastern North Carolina and South Carolina (portions of 231I–Central Appalachian Piedmont, 232C–Atlantic Coastal Flatwoods, 232H–Middle Atlantic Coastal Plains and Flatwoods, and 232I–Northern Atlantic Coastal Flatwoods). Although no specific forest health impacts have been reported in these areas, recent evidence suggests a link between persistent excess moisture and increased vulnerability of forests to pathogens and other disease-causing agents (Hubbart and others 2016). These agents may be further enabled during times of high climate variability, such as when a period of drought occurs immediately before or after a period of moisture surplus (Hubbart and others 2016). A pertinent geographic example is eastern Texas, which saw multiple areas of moderate to extreme moisture surplus during the 2013–2017 period (in portions of 231E–Mid Coastal Plains-Western, 232F–Coastal Plains and Flatwoods-Western Gulf, 255B–Blackland Prairies, and 255C–Oak Woods and Prairies; see fig. 4.5). Notably, this prolonged period of surplus came shortly after Texas experienced its worst 1-year drought on record in 2011, which resulted in estimated mortality of >6 percent of forest trees statewide, roughly nine times the normal background mortality (Moore and others 2016). Forests in this region should be monitored over the next several years for possible impacts related to this pronounced swing in moisture conditions. Monitoring may also be advisable for the three areas of moisture surplus identified above (i.e., the western Great Lakes region, Kentucky and southern Indiana, and the Carolinas). These areas were less extensive in the 3-year *MDZ* map than in the 5-year map, which may be a preliminary signal of a shift from surplus to drought conditions in some locations.

Future Efforts

We intend to produce 1-year, 3-year, and 5-year *MDZ* maps of the conterminous United States as a regular yearly component of national-scale forest health reporting. To interpret the maps appropriately, it is important to recognize their limitations. Foremost, the *MDZ* approach does not incorporate some factors that may affect a location's moisture supply at a finer spatial scale, such as winter snowpack, surface runoff, or groundwater storage. Furthermore, although the maps use a standardized index scale that applies regardless of the size of the time window, the window size may still merit consideration. For example, an extreme drought that persists for 5 years has substantially different forest health implications than an extreme drought that lasts only a single year. Together, the 1-year, 3-year, and 5-year *MDZ* maps provide a comprehensive short-term overview, but a region's longer term moisture history may also be meaningful with respect to the health of its forests. For instance, in regions where droughts have been frequent historically (e.g., occurring on an annual or nearly annual basis), some tree species may be better drought-adapted than others (McDowell and others 2008). Because of this variability in species' drought resistance, a long period of persistent and severe drought conditions could ultimately lead to changes in regional forest composition (Mueller and others 2005); compositional changes similarly may arise from a long period of persistent moisture surplus (McEwan and others 2011). In turn, such changes are likely to affect regional responses to future drought or surplus conditions, fire regimes, and the status of ecosystem services such as nutrient cycling and wildlife habitat (W.R.L. Anderegg and others 2013, DeSantis and others 2011). In future work, we hope to provide forest managers and other decisionmakers with better quantitative evidence regarding critical relationships between moisture extremes and significant forest health impacts such as regional-scale tree mortality (e.g., Mitchell and others 2014). We also intend to examine the capacity of moisture extremes to serve as inciting factors for other forest threats such as wildfire or pest outbreaks.

LITERATURE CITED

Adams, H.D.; Guardiola-Claramonte, M.; Barron-Gafford, G.A. [and others]. 2009. Temperature sensitivity of drought-induced tree mortality portends increased regional die-off under global-change-type drought. Proceedings of the National Academy of Sciences. 106(17): 7063–7066.

Akin, W.E. 1991. Global patterns: climate, vegetation, and soils. Norman, OK: University of Oklahoma Press. 370 p.

Allen, C.D.; Macalady, A.K.; Chenchouni, H. [and others]. 2010. A global overview of drought and heat-induced tree mortality reveals emerging climate change risks for forests. Forest Ecology and Management. 259(4): 660–684.

Alley, W.M. 1984. The Palmer Drought Severity Index: limitations and assumptions. Journal of Climate and Applied Meteorology. 23: 1100–1109.

Anderegg, L.D.L.; Anderegg, W.R.L.; Berry, J.A. 2013. Not all droughts are created equal: translating meteorological drought into woody plant mortality. Tree Physiology. 33(7): 672–683.

Anderegg, W.R.L.; Kane, J.M.; Anderegg, L.D.L. 2013. Consequences of widespread tree mortality triggered by drought and temperature stress. Nature Climate Change. 3(1): 30–36.

Archaux, F.; Wolters, V. 2006. Impact of summer drought on forest biodiversity: what do we know? Annals of Forest Science. 63: 645–652.

Berdanier, A.B.; Clark, J.S. 2016. Multiyear drought-induced morbidity preceding tree death in southeastern U.S. forests. Ecological Applications. 26(1): 17–23.

Clark, J.S. 1989. Effects of long-term water balances on fire regime, north-western Minnesota. Journal of Ecology. 77: 989–1004.

Cleland, D.T.; Freeouf, J.A.; Keys, J.E. [and others]. 2007. Ecological subregions: sections and subsections for the conterminous United States. Gen. Tech. Report WO-76D. Washington, DC: U.S. Department of Agriculture Forest Service. Map; Sloan, A.M., cartographer; presentation scale 1:3,500,000; colored. Also on CD-ROM as a GIS coverage in ArcINFO format or at http://data.fs.usda.gov/geodata/edw/datasets.php. [Date accessed: July 20, 2015].

Clinton, B.D.; Boring, L.R.; Swank, W.T. 1993. Canopy gap characteristics and drought influences in oak forests of the Coweeta Basin. Ecology. 74(5): 1551–1558.

Daly, C.; Gibson, W.P.; Taylor, G.H. [and others]. 2002. A knowledge-based approach to the statistical mapping of climate. Climate Research. 22: 99–113.

DeSantis, R.D.; Hallgren, S.W.; Stahle, D. W. 2011. Drought and fire suppression lead to rapid forest composition change in a forest-prairie ecotone. Forest Ecology and Management. 261(11): 1833–1840.

Duever, M.J.; Meeder, J.F.; Meeder, L.C.; McCollum, J.M. 1994. The climate of south Florida and its role in shaping the Everglades ecosystem. In: Davis, S.M.; Ogden, J.C., eds. Everglades: the ecosystem and its restoration. Delray Beach, FL: St. Lucie Press: 225–248.

Gil-Alana, L.A. 2018. Maximum and minimum temperatures in the United States: time trends and persistence. Atmospheric Science Letters. 19(4): e810.

Groisman, P.Y.; Knight, R.W. 2008. Prolonged dry episodes over the conterminous United States: new tendencies emerging during the last 40 years. Journal of Climate. 21: 1850–1862.

Grundstein, A. 2009. Evaluation of climate change over the continental United States using a moisture index. Climatic Change. 93: 103–115.

Guarín, A.; Taylor, A.H. 2005. Drought triggered tree mortality in mixed conifer forests in Yosemite National Park, California, USA. Forest Ecology and Management. 218: 229–244.

Hanson, P.J.; Weltzin, J.F. 2000. Drought disturbance from climate change: response of United States forests. Science of the Total Environment. 262: 205–220.

Hubbart, J.A.; Guyette, R.; Muzika, R.-M. 2016. More than drought: precipitation variance, excessive wetness, pathogens and the future of the western edge of the Eastern Deciduous Forest. Science of the Total Environment. 566–567: 463–467.

Kareiva, P.M.; Kingsolver, J.G.; Huey, B.B., eds. 1993. Biotic interactions and global change. Sunderland, MA: Sinauer Associates, Inc. 559 p.

Keetch, J.J.; Byram, G.M. 1968. A drought index for forest fire control. Asheville, NC: U.S. Department of Agriculture Forest Service, Southeastern Forest Experiment Station. 33 p.

Koch, F.H.; Coulston, J.W. 2015. One-year (2013), three-year (2011–2013), and five-year (2009–2013) drought maps for the conterminous United States. In: Potter, K.M.; Conkling, B.L., eds. Forest Health Monitoring: national status, trends, and analysis 2014. Gen. Tech. Rep. SRS-209. Asheville, NC: U.S. Department of Agriculture Forest Service, Southern Research Station: 57–71. Chapter 4.

Koch, F.H.; Coulston, J.W. 2016. 1-year (2014), 3-year (2012–2014), and 5-year (2010–2014) maps of drought and moisture surplus for the conterminous United States. In: Potter, K.M.; Conkling, B.L., eds. Forest Health Monitoring: national status, trends, and analysis 2015. Gen. Tech. Rep. SRS-213. Asheville, NC: U.S. Department of Agriculture Forest Service, Southern Research Station: 61–78. Chapter 4.

Koch, F.H.; Coulston, J.W. 2017. Moisture deficit and surplus in the conterminous United States for three time windows: 2015, 2013–2015, and 2011–2015. In: Potter, K.M.; Conkling, B.L., eds. Forest Health Monitoring: national status, trends, and analysis 2016. Gen. Tech. Rep. SRS-222. Asheville, NC: U.S. Department of Agriculture Forest Service, Southern Research Station: 63–80. Chapter 4.

Koch, F.H.; Coulston, J.W. 2018. Moisture deficit and surplus in the conterminous United States for three time windows: 2016, 2014–2016, and 2012–2016. In: Potter, K.M.; Conkling, B.L., eds. Forest Health Monitoring: national status, trends, and analysis 2017. Gen. Tech Rep. SRS-233. Asheville, NC: U.S. Department of Agriculture Forest Service, Southern Research Station: 65–84. Chapter 4.

Koch, F.H.; Coulston, J.W.; Smith, W.D. 2012a. High-resolution mapping of drought conditions. In: Potter, K.M.; Conkling, B.L., eds. Forest Health Monitoring 2008 national technical report. Gen. Tech. Rep. SRS-158. Asheville, NC: U.S. Department of Agriculture Forest Service, Southern Research Station: 45–62. Chapter 4.

Koch, F.H.; Coulston, J.W.; Smith, W.D. 2012b. Mapping drought conditions using multi-year windows. In: Potter, K.M.; Conkling, B.L., eds. Forest Health Monitoring 2009 national technical report. Gen. Tech. Rep. SRS-167. Asheville, NC: U.S. Department of Agriculture Forest Service, Southern Research Station: 163–179. Chapter 10.

Koch, F.H.; Smith, W.D.; Coulston, J.W. 2013a. Recent drought conditions in the conterminous United States. In: Potter, K.M.; Conkling, B.L., eds. Forest Health Monitoring: national status, trends, and analysis 2011. Gen. Tech. Rep. SRS-185. Asheville, NC: U.S. Department of Agriculture Forest Service, Southern Research Station: 41–58. Chapter 4.

Koch, F.H.; Smith, W.D.; Coulston, J.W. 2013b. An improved method for standardized mapping of drought conditions. In: Potter, K.M.; Conkling, B.L., eds. Forest Health Monitoring: national status, trends, and analysis 2010. Gen. Tech. Rep. SRS-176. Asheville, NC: U.S. Department of Agriculture Forest Service, Southern Research Station: 67–83. Chapter 6.

Koch, F.H.; Smith, W.D.; Coulston, J.W. 2014. Drought patterns in the conterminous United States and Hawaii. In: Potter, K.M.; Conkling, B.L., eds. Forest Health Monitoring: national status, trends, and analysis 2012. Gen. Tech. Rep. SRS-198. Asheville, NC: U.S. Department of Agriculture Forest Service, Southern Research Station: 49–72. Chapter 4.

Koch, F.H.; Smith, W.D.; Coulston, J.W. 2015. Drought patterns in the conterminous United States, 2012. In: Potter, K.M.; Conkling, B.L., eds. Forest Health Monitoring: national status, trends, and analysis 2013. Gen. Tech. Rep. SRS-207. Asheville, NC: U.S. Department of Agriculture Forest Service, Southern Research Station: 55–69. Chapter 4.

Kolb, T.E.; Fettig, C.J.; Ayres, M.P. [and others]. 2016. Observed and anticipated impacts of drought on forest insects and diseases in the United States. Forest Ecology and Management. 380: 321–334.

Laurance, S.G.W.; Laurance, W.F.; Nascimento, H.E.M. [and others]. 2009. Long-term variation in Amazon forest dynamics. Journal of Vegetation Science. 20(2): 323–333.

Lesk, C.; Coffel, E.; D'Amato, A.W. [and others]. 2017. Threats to North American forests from southern pine beetle with warming winters. Nature Climate Change. 7: 713.

Marlier, M.E.; Xiao, M.; Engel, R. [and others]. 2017. The 2015 drought in Washington State: a harbinger of things to come? Environmental Research Letters. 12(11): 114008.

Martínez-Vilalta, J.; Lloret, F.; Breshears, D.D. 2012. Drought-induced forest decline: causes, scope and implications. Biology Letters. 8(5): 689–691.

Mattson, W.J.; Haack, R.A. 1987. The role of drought in outbreaks of plant-eating insects. BioScience. 37(2): 110–118.

McDowell, N.; Pockman, W.T.; Allen, C.D. [and others]. 2008. Mechanisms of plant survival and mortality during drought: why do some plants survive while others succumb to drought? New Phytologist. 178: 719–739.

McEwan, R.W.; Dyer, J.M.; Pederson, N. 2011. Multiple interacting ecosystem drivers: toward an encompassing hypothesis of oak forest dynamics across eastern North America. Ecography. 34: 244–256.

McKee, T.B.; Doesken, N.J.; Kleist, J. 1993. The relationship of drought frequency and duration to time scales. In: Eighth conference on applied climatology. American Meteorological Society: 179–184.

Millar, C.I.; Westfall, R.D.; Delany, D.L. 2007. Response of high-elevation limber pine (*Pinus flexilis*) to multiyear droughts and 20th-century warming, Sierra Nevada, California, USA. Canadian Journal of Forest Research. 37: 2508–2520.

Mitchell, P.J.; O'Grady, A.P.; Hayes, K.R.; Pinkard, E.A. 2014. Exposure of trees to drought-induced die-off is defined by a common climatic threshold across different vegetation types. Ecology and Evolution. 4(7): 1088–1101.

Monteith, J.L. 1965. Evaporation and environment. Symposia of the Society for Experimental Biology. 19: 205–234.

Moore, G.W.; Edgar, C.B.; Vogel, J.G. [and others]. 2016. Tree mortality from an exceptional drought spanning mesic to semiarid ecoregions. Ecological Applications. 26(2): 602–611.

Mueller, R.C.; Scudder, C.M.; Porter, M.E. [and others]. 2005. Differential tree mortality in response to severe drought: evidence for long-term vegetation shifts. Journal of Ecology. 93: 1085–1093.

National Climatic Data Center. 2018a. Climatological rankings - temperature, precipitation, and drought. http://www.ncdc.noaa.gov/temp-and-precip/climatological-rankings/index.php. [Date accessed: September 12, 2018].

National Climatic Data Center. 2018b. State of the climate - drought - annual report 2017. https://www.ncdc.noaa.gov/sotc/drought/201713. [Date accessed: September 10, 2018].

Palmer, W.C. 1965. Metereological drought. Washington, DC: U.S. Department of Commerce, Weather Bureau. 58 p.

Peng, C.; Ma, Z.; Lei, X. [and others]. 2011. A drought-induced pervasive increase in tree mortality across Canada's boreal forests. Nature Climate Change. 1(9): 467–471.

Peters, M.P.; Iverson, L.R.; Matthews, S.N. 2015. Long-term droughtiness and drought tolerance of eastern US forests over five decades. Forest Ecology and Management. 345: 56–64.

Potter, C.S.; Klooster, S.A. 1999. Dynamic global vegetation modelling for prediction of plant functional types and biogenic trace gas fluxes. Global Ecology and Biogeography. 8(6): 473–488.

PRISM Climate Group. 2018. 2.5-arcmin (4 km) gridded monthly climate data. http://www.prism.oregonstate.edu. [Date accessed: June 14, 2018].

Raffa, K.F.; Aukema, B.H.; Bentz, B.J. [and others]. 2008. Cross-scale drivers of natural disturbances prone to anthropogenic amplification: the dynamics of bark beetle eruptions. BioScience. 58(6): 501–517.

Rahmstorf, S.; Foster, G.; Cahill, N. 2017. Global temperature evolution: recent trends and some pitfalls. Environmental Research Letters. 12(5): 054001.

Rozas, V.; García-González, I. 2012. Too wet for oaks? Inter-tree competition and recent persistent wetness predispose oaks to rainfall-induced dieback in Atlantic rainy forest. Global and Planetary Change. 94–95: 62–71.

Rozas, V.; Sampedro, L. 2013. Soil chemical properties and dieback of *Quercus robur* in Atlantic wet forests after a weather extreme. Plant and Soil. 373(1–2): 673–685.

Schoennagel, T.; Veblen, T.T.; Romme, W.H. 2004. The interaction of fire, fuels, and climate across Rocky Mountain forests. BioScience. 54(7): 661–676.

Steinemann, A. 2003. Drought indicators and triggers: a stochastic approach to evaluation. Journal of the American Water Resources Association. 39(5): 1217–1233.

Svoboda, M.; LeComte, D.; Hayes, M. [and others]. 2002. The Drought Monitor. Bulletin of the American Meteorological Society. 83(8): 1181–1190.

Sweet, S.K.; Wolfe, D.W.; DeGaetano, A.; Benner, R. 2017. Anatomy of the 2016 drought in the Northeastern United States: implications for agriculture and water resources in humid climates. Agricultural and Forest Meteorology. 247: 571–581.

Thornthwaite, C.W. 1948. An approach towards a rational classification of climate. Geographical Review. 38(1): 55–94.

Thornthwaite, C.W.; Mather, J.R. 1955. The water balance. Publications in Climatology. 8(1): 1–104.

Trouet, V.; Taylor, A.H.; Wahl, E.R. [and others]. 2010. Fire-climate interactions in the American West since 1400 CE. Geophysical Research Letters. 37(4): L04702.

USDA Forest Service Region 5 Forest Health Monitoring program. 2018. 2017 aerial survey results: California. Press Rel. R5-PR-034. Davis, CA: U.S. Department of Agriculture Forest Service, Pacific Southwest Region. 18 p.

Vose, R.S.; Applequist, S.; Squires, M. [and others]. 2014. Improved historical temperature and precipitation time series for U.S. climate divisions. Journal of Applied Meteorology and Climatology. 53(5): 1232–1251.

Williams, A.P.; Allen, C.D.; Macalady, A.K. [and others]. 2013. Temperature as a potent driver of regional forest drought stress and tree mortality. Nature Climate Change. 3(3): 292–297.

Willmott, C.J.; Feddema, J.J. 1992. A more rational climatic moisture index. Professional Geographer. 44(1): 84–87.

Woodhouse, C.A.; Meko, D.M.; MacDonald, G.M. [and others]. 2010. A 1,200-year perspective of 21st century drought in southwestern North America. Proceedings of the National Academy of Sciences. 107(50): 21283–21288.